








Tumor microenvironment shows an immunological abscopal effect in patients with NSCLC treated with pembrolizumab-radiotherapy combination

Lieke L van der Woude ^{1,2,3} Mark A J Gorris ^{1,3} Inge M N Wortel,⁴
Jeroen H A Creemers ^{1,3} Kiek Verrijp ^{1,2,3} Kim Monkhorst,⁵
Katrien Grünberg,² Michel M van den Heuvel,⁶ Johannes Textor ^{1,4}
Carl G Figdor ¹ Berber Piet,⁶ Willemijn S M E Theelen,⁷ I Jolanda M de Vries ¹

To cite: van der Woude LL, Gorris MAJ, Wortel IMN, *et al*. Tumor microenvironment shows an immunological abscopal effect in patients with NSCLC treated with pembrolizumab-radiotherapy combination. *Journal for ImmunoTherapy of Cancer* 2022;**10**:e005248. doi:10.1136/jitc-2022-005248

► Additional supplemental material is published online only. To view, please visit the journal online (<http://dx.doi.org/10.1136/jitc-2022-005248>).

BP, WSMET and IJMdV are joint senior authors.

Accepted 17 September 2022



© Author(s) (or their employer(s)) 2022. Re-use permitted under CC BY-NC. No commercial re-use. See rights and permissions. Published by BMJ.

For numbered affiliations see end of article.

Correspondence to

Professor I Jolanda M de Vries; jolanda.devries@radboudumc.nl

ABSTRACT

Background Immunotherapy is currently part of the standard of care for patients with advanced-stage non-small cell lung cancer (NSCLC). However, many patients do not respond to this treatment, therefore combination strategies are being explored to increase clinical benefit. The PEMBRO-RT trial combined the therapeutic programmed cell death 1 (PD-1) antibody pembrolizumab with stereotactic body radiation therapy (SBRT) to increase the overall response rate and study the effects on the tumor microenvironment (TME).

Methods Here, immune infiltrates in the TME of patients included in the PEMBRO-RT trial were investigated. Tumor biopsies of patients treated with pembrolizumab alone or combined with SBRT (a biopsy of the non-irradiated site) at baseline and during treatment were stained with multiplex immunofluorescence for CD3, CD8, CD20, CD103 and FoxP3 for lymphocytes, pan-cytokeratin for tumors, and HLA-ABC expression was determined.

Results The total number of lymphocytes increased significantly after 6 weeks of treatment in the anti-PD-1 group (fold change: 1.87, 95% CI: 1.06 to 3.29) and the anti-PD-1+SBRT group (fold change: 2.29, 95% CI: 1.46 to 3.60). The combination of SBRT and anti-PD-1 induced a 4.87-fold increase (95% CI: 2.45 to 9.68) in CD103⁺ cytotoxic T-cells 6 weeks on treatment and a 2.56-fold increase (95% CI: 1.03 to 6.36) after anti-PD-1 therapy alone. Responders had a significantly higher number of lymphocytes at baseline than non-responders (fold difference 1.85, 95% CI: 1.04 to 3.29 for anti-PD-1 and fold change 1.93, 95% CI: 1.08 to 3.44 for anti-PD-1+SBRT).

Conclusion This explorative study shows that that lymphocyte infiltration in general, instead of the infiltration of a specific lymphocyte subset, is associated with response to therapy in patients with NSCLC. Furthermore, anti-PD-1+SBRT combination therapy induces an immunological abscopal effect in the TME represented by a superior infiltration of cytotoxic T cells as compared with anti-PD-1 monotherapy.

WHAT IS ALREADY KNOWN ON THIS TOPIC

⇒ Immunotherapy and stereotactic body radiation therapy (SBRT) combined increased the overall response rate compared with immunotherapy alone in patients with metastatic non-small cell lung cancer in the PEMBRO-RT study (NCT02492568).

WHAT THIS STUDY ADDS

⇒ The presence of high numbers of lymphocytes in the TME before treatment is associated with response to immunotherapy and SBRT in patients with lung cancer.
⇒ The addition of SBRT to immunotherapy increases the number of lymphocytes within the TME of non-irradiated tumor sites in patients with lung cancer.

HOW THIS STUDY MIGHT AFFECT RESEARCH, PRACTICE OR POLICY

⇒ Understanding the immunological abscopal effect in the TME may lead to better therapeutic options for patients who do not respond to combination therapy.

BACKGROUND

The recent introduction of immunotherapy has greatly improved clinical outcomes for a subset of patients with non-small cell lung cancer (NSCLC), as evidenced by long-lasting responses.^{1 2} Immunotherapy targeting the programmed death-ligand 1 (PD-L1)/programmed cell death 1 (PD-1) pathway, also known as immune checkpoint inhibition (ICI), with or without chemotherapy, is now the standard of care treatment for patients with advanced NSCLC without actionable targets.^{3–5} Unfortunately, many patients with NSCLC do not respond to ICI therapy.⁶ One of the biggest challenges lies in finding solutions for non-responding patients.

Radiotherapy currently has an essential role in the treatment of symptoms in advanced NSCLC. In addition, historical evidence suggests that radiotherapy can influence the anticancer immune response. Incidental instances of an abscopal effect, whereby irradiating one tumor lesion leads to the shrinkage or disappearance of other tumor lesions,⁷ have led to a new avenue of investigations into the synergistic possibilities of combining immunotherapy with radiotherapy.

The underlying mechanism for an abscopal effect of radiotherapy, based on preclinical models, might be the release of double-stranded DNA and RNA activating the 'stimulator of interferon (IFN) genes' signaling pathway in dendritic cells (DCs) through type I IFN-driven immune activation. Recruited DCs can take up tumor antigens, migrate to lymph nodes and (cross-)present antigens to T-cells. These T-cells can migrate to the tumor, infiltrate the tumor microenvironment (TME) and kill tumor cells.^{8–10} Radiotherapy can also influence myeloid-derived suppressor cells (MDSCs), drive pro-inflammatory macrophage polarization and increase PD-L1 expression in tumors.^{11–14} Furthermore, radiotherapy can upregulate major histocompatibility complex (MHC) class I expression.^{8,15} Combination of anti-PD-1 treatment with radiation therapy might therefore be beneficial for immune recognition via MHC class I.

In the randomized PEMBRO-RT trial (NCT02492568),¹⁶ stereotactic body radiotherapy (SBRT) to a single tumor lesion preceding pembrolizumab treatment increased the overall response rate (ORR) from 18% to 36% compared with pembrolizumab alone in patients with metastatic NSCLC, thereby confirming the previously formulated hypotheses in a randomized fashion.^{17,18} However, it remains unclear through which mechanisms SBRT affects the anti-cancer immune response when combined with pembrolizumab.

We explore the difference in immune cell composition within the TME of patients from the PEMBRO-RT trial treated with pembrolizumab with or without SBRT. Multiplex immunofluorescence (mIF) with automated quantitative image analysis conserving spatial and architectural information is used to study different immune cell populations within the TME of these patients. Insight into how SBRT on one lesion alters the TME immune composition of other, distant lesions in pembrolizumab-treated patients can increase our understanding of the mechanisms behind improved therapy response, with the ultimate goal to increase the clinical benefit of immunotherapy for patients with NSCLC.

MATERIALS AND METHODS

Patient material

Tumor material was collected from patients with stage IV NSCLC treated within the PEMBRO-RT study (NCT02492568),¹⁶ who received either pembrolizumab alone (anti-PD-1 group) or pembrolizumab combined with SBRT (anti-PD-1+SBRT group). On-treatment

samples were collected 6 weeks after the start of pembrolizumab and were obtained from a non-irradiated site (online supplemental figure 1). Note that, as overall survival 6 weeks after treatment was still >95% in this trial, any differences found between baseline and on-treatment samples in this study are unlikely to result from a survivor's bias.

Tumor tissue was collected based on accessibility for biopsy. All biopsies were collected from tumor locations outside the radiotherapy field. On-treatment biopsies were obtained from the same lesion as the biopsy obtained at baseline. The samples were collected at the Netherlands Cancer Institute, Erasmus Medical Center and the VU University Medical Center. The trial was conducted in accordance with the provisions of the Declaration of Helsinki¹⁹ and the Good Clinical Practice guidelines of the European Medicines Agency and the US Food and Drug Administration.

Patient samples and characteristics

Biopsy material was available for 62 out of the 76 patients treated in the PEMBRO-RT trial.¹⁶ Samples were evaluated for quality and excluded if no sufficient tumor material was present. After quality assessment, baseline biopsy material from 56 patients was suitable and selected for further analysis (27 in the anti-PD-1+SBRT group and 29 in the anti-PD-1 group). In the anti-PD-1+SBRT group, 15 matched (baseline and on-treatment) and 3 on-treatment only biopsies were of adequate quality. In this group, biopsies were taken from tumors that were not irradiated. In the anti-PD-1 group, there were 13 matched and 3 on-treatment only biopsies. Due to insufficient tumor biopsy material, HLA-ABC was determined on 24 baseline samples and 16 on-treatment samples in the anti-PD-1+SBRT group. Similarly, 27 baseline samples and 15 on-treatment samples in the anti-PD-1 group were stained and analyzed for HLA-ABC. For several patients, paired samples were not available. To prevent loss of data and selection bias, unpaired analysis, including all available data, was performed.

Patient characteristics of the 62 patients from the PEMBRO-RT cohort with available biopsy material are provided in [table 1](#). Patients with NSCLC with an adenocarcinoma (n=48), squamous cell carcinoma (n=9) and large-cell neuroendocrine tumors (n=4) were included. Groups were comparable in sex, age and smoking status (see [table 1](#)). In the anti-PD-1 group, the PD-L1 status was missing for one patient. The anti-PD-1+SBRT group had slightly more patients with a PD-L1 tumor proportion score of 50% or higher than the anti-PD-1 group (23% vs 13%) and also more patients with PD-L1 expression $\geq 1\%$ (43% vs 30%).

Multiplex immunohistochemistry

Formalin-fixed and paraffin-embedded tumor samples were sectioned at 4 μm thickness and mounted onto Superfrost PLUS slides (900226, VWR). Slides were stained using the Bond RX autostainer (Leica Biosystems)

Table 1 Patient characteristics of the study cohort of 62 patients with available biopsy material

	α PD-1+SBRT n (%)	α PD-1 n (%)	Total n (%)
Sex			
Male	16 (53)	19 (60)	35 (57)
Female	14 (47)	13 (40)	27 (43)
Age			
In years at randomization (range)	61 (35–75)	62 (38–78)	61 (35–78)
Smoking			
Current	7 (23)	3 (10)	10 (16)
Former	20 (67)	26 (84)	46 (76)
Never	3 (10)	2 (6)	5 (8)
> 10 pack-year	24 (80)	25 (80)	49 (80)
Histology			
AC	23 (77)	26 (81)	49 (79)
SCC	5 (17)	4 (13)	9 (15)
LCNEC	2 (6)	2 (6)	4 (6)
Baseline PD-L1 TPS			
0	17 (57)	22 (70)	39 (64)
1–49	6 (20)	5 (17)	11 (18)
≥50	7 (23)	4 (13)	11 (18)
Best overall response			
PD	12 (40)	18 (56)	30 (48)
SD	4 (13)	8 (25)	12 (19)
PR	11 (37)	5 (16)	16 (26)
CR	3 (10)	1 (3)	4 (7)

Numbers represent n (%) and for age median age in years at randomization (range).
 AC, adenocarcinoma; CR, complete response; LCNEC, large cell neuroendocrine carcinoma; PD, progressive disease; PD-1, programmed cell death 1; PD-L1, programmed death-ligand 1; PR, partial response; SBRT, stereotactic body radiation therapy; SCC, squamous cell carcinoma; SD, stable disease; TPS, tumor proportion score.

with one seven-color mIF panel and one three-color mIF panel using the Opal 7-color Automation IHC Kit (NEL801001KT; PerkinElmer). The order of antibody/opal staining cycles was optimized for lung cancer tissue using a previously developed optimization protocol.²⁰

Slides were deparaffinized with Bond dewax solution (AR9222, Leica Biosystems). Epitope retrieval was achieved by heating the slides to 95°C and incubating them with Bond Epitope Retrieval 2 (AR9640, Leica Biosystems) for 20 min. Blocking was performed with antibody diluent (Opal kit NEL801001KT; PerkinElmer) for 10 min at room temperature. Primary antibody incubations were performed for 1 hour at room temperature. Secondary antibody (Opal kit NEL801001KT;

PerkinElmer) incubations were performed for 30 min at room temperature.

The first seven-color mIF ‘lymphocyte’ panel was stained with the following antibody/opal combination; anti-CD8 (Dako, M7103, clone C8/144B, 1:100) and Opal690, anti-CD20 (ThermoFisher, MS-340, clone L26, 1:600) and Opal570, anti-CD3 (ThermoFisher, clone RM-9107, 1:200) and Opal520, anti-CD103 (Cell Marque, 437R-14, clone EP206, 1:50) and Opal620, anti-FOXP3 (eBioscience Affymetrix, 14-4777, clone 236A/E7, 1:100) and Opal540, anti-pan-cytokeratin (Abcam ab86734, clone AE1/AE3+5D3, 1:500) and Opal650.

The second three-color mIF ‘tumor’ panel was stained with the following antibody/opal combination: anti-HLA-ABC (Abcam, ab70328, clone EMR8-5, 1:1000) and Opal520, anti-indoleamine 2,3-dioxygenase (IDO) (EMD Millipore, MAB10009, clone IF8-2, 1:100) and Opal570, anti-pan-cytokeratin (Abcam ab86734, clone AE1/AE3+5D3, 1:500) and Opal650. After quality assessment, the IDO staining was of insufficient quality and discarded for further analysis. All tissue sections were manually counterstained with 4',6-diamidino-2-phenylindole (DAPI) and mounted with Fluoromount-G (0100-01; Southern Biotech).

Tissue imaging, segmentation and analysis

Slides were scanned using the Automated Quantitative Pathology Imaging System (Vectra V.3.0.4, PerkinElmer) at an overview (4× magnification). Phenochart (V.1.0.9, PerkinElmer) was used to annotate multispectral images of tumor tissue to be scanned at 20× magnification. InForm software (V.2.4.2, PerkinElmer) was used for spectral unmixing of Opal fluorophores. Spectral unmixed images were digitally merged to create high magnification overviews of the tissue slides. Samples were assessed by a pathologist (ML/KG), and a region of interest (ROI) was selected containing the tumor and all surrounding stroma. Healthy tissue surrounding the tumor was excluded from the ROI. Tissue was segmented using inForm software to identify tumor regions (pan-cytokeratin positive areas). Due to the nature of the available tissue (ie, most samples were small biopsies), it was not possible to reliably identify an invasive margin, therefore we analyzed the lymphocyte infiltration per sample and no further distinction between tumor infiltrating lymphocytes or tumor excluded lymphocytes was made. HLA-ABC staining was converted to pseudo-3,3'-diaminobenzidine staining and scored for the absence of membranous expression of HLA-ABC.

Automated detection of immune cell types

Because the inForm software cannot always reliably assign immune cell types in dense tissues such as tumors, immune cell phenotypes were instead identified using a neural network called ImmuNet. Details are described in the ImmuNet preprint.²¹ The version of ImmuNet used to detect lymphocytes and the input images/ROIs will be deposited on Zenodo on acceptance of this manuscript.

To assess the accuracy of the network on the current dataset, 140 small ROIs were selected on the whole slide images and fully annotated by human specialists. Then, for each ROI, the number of annotated cells was compared with the number of cells detected by ImmuNet. The agreement between these annotations and the network prediction was determined using the intraclass correlation coefficient (ICC, computed using the 'icc' function of R package 'irr' (v0.84.1)²² with model='twoway', type='agreement', unit='single').

Lymphocytes identified by the neural network were converted to densities per ROI (cells/mm²), saved in Flow Cytometry Standard files and further phenotyped using FlowJo software (V.10; Tree Star; online supplemental figure 2).

Statistical analysis

Statistical analysis and data visualization of results was performed with R (V.4.0.5, RRID

SCR_001905) and PRISM 8 (GraphPad, GSL Biotech, California, USA).

For principal component analysis (PCA), lymphocyte densities were log-transformed (adding 0.1 to the raw densities to avoid problems when log-transforming zero densities). PCA was performed using R's 'princomp' function (default settings). Responders and non-responders in PCA plots were compared in two ways: (1) by plotting 95% confidence regions (based on the covariance matrix of the first two principal components (PCs)) for each group using R's 'ellipse' package (V.0.4.2) and (2) by performing a Welch's two-sample t-test on the PC1 scores ('t.test' function in R with default settings). Note that both these comparison methods only yield rough estimates because they falsely assume that input data points are independent of each other (all data influence the PC loadings and thus their PC scores). We report these metrics here as a rough indication, but they should be interpreted with caution as they may differ (slightly) from the actual p values and confidence regions.

Data were plotted in graphics resembling the Gardner-Altman plot to compare lymphocyte densities between baseline and on-treatment samples, or between responders and non-responders.²³ These plots show both the groupwise lymphocyte densities and the 95% CI of the fold change between groups (derived from a Welch's two-sample 't.test' in R on the log-transformed lymphocyte densities).

The linear (Pearson's) correlation coefficient was measured between the log-transformed densities to assess correlations between lymphocyte (sub)populations.

Due to the explorative nature of this study, no correction for multiple testing was applied.

RESULTS

A computational neural network detects lymphocyte populations in the tumor microenvironment of patients with NSCLC

To investigate the TME composition within patient samples at baseline and after 6 weeks of treatment, an mIF

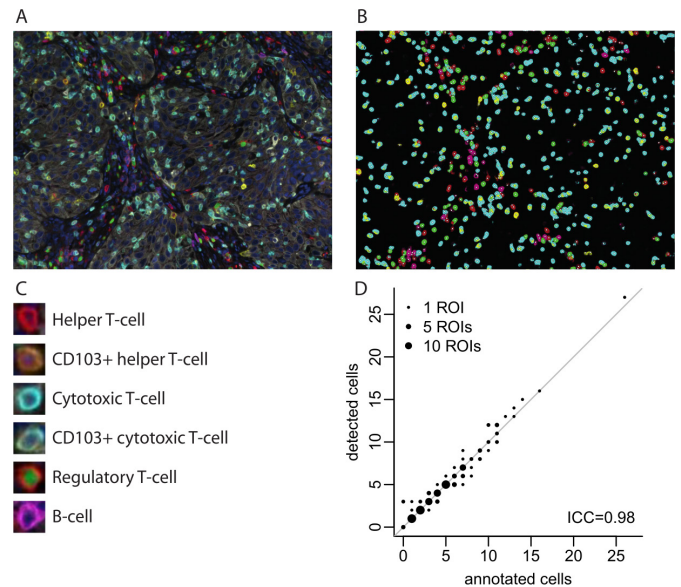


Figure 1 Analysis of multiplex immunofluorescence images and lymphocyte subsets using a custom neural network. (A) Multispectral image at 20× magnification stained with multiplex panel containing CD3, CD8, CD20, CD103 and FoxP3. (B) Image after immune cell detection with a neural network. (C) Overview of lymphocyte subsets. (D) Accuracy of neural network in detecting T-cells and B-cells. ICC, intraclass correlation coefficient; ROI, region of interest.

panel was developed containing six markers and DAPI. This panel enabled the identification of six lymphocyte subsets: helper T-cells, CD103⁺ helper T-cells, cytotoxic T-cells, CD103⁺ cytotoxic T-cells, regulatory T-cells and B-cells (figure 1A,B). CD3⁺ CD8⁻ FoxP3⁻ cells are regarded as T helper cells. The presence of NKT cells or double negative TILs within this CD3⁺ CD8⁻ FoxP3⁻ population is considered neglectable since these cells are, in NSCLC tissue, only present in minute numbers (0.39%–1.4% of lymphocytes).^{24,25} Integrin CD103 is a marker for tissue-resident T cells and was used to identify intra-epithelial T-cells.²⁶ Lymphocytes were identified using ImmuNet, a computational neural network developed to detect the lymphocytes stained with this mIF panel (figure 1C).²¹ The accuracy of the neural network for identifying lymphocytes in this dataset was determined (ICC=0.98, figure 1D). Analysis of the whole ROI, containing both tumor and stroma, or only the segmented tumor region showed similar outcomes (data not shown). For simplicity, all downstream analyses are therefore based on the whole ROI.

Total lymphocyte infiltration, but not specific lymphocyte subset infiltration at baseline, is associated with response to therapy

The immune cell density within the TME can vary extensively, as shown in figure 2A,B. Furthermore, it has previously been associated with response to ICI.²⁷ In our cohort, both treatment groups had similar amounts of lymphocytes at baseline (online supplemental figure 3). As can be seen in table 1, the anti-PD-1+SBRT group had slightly

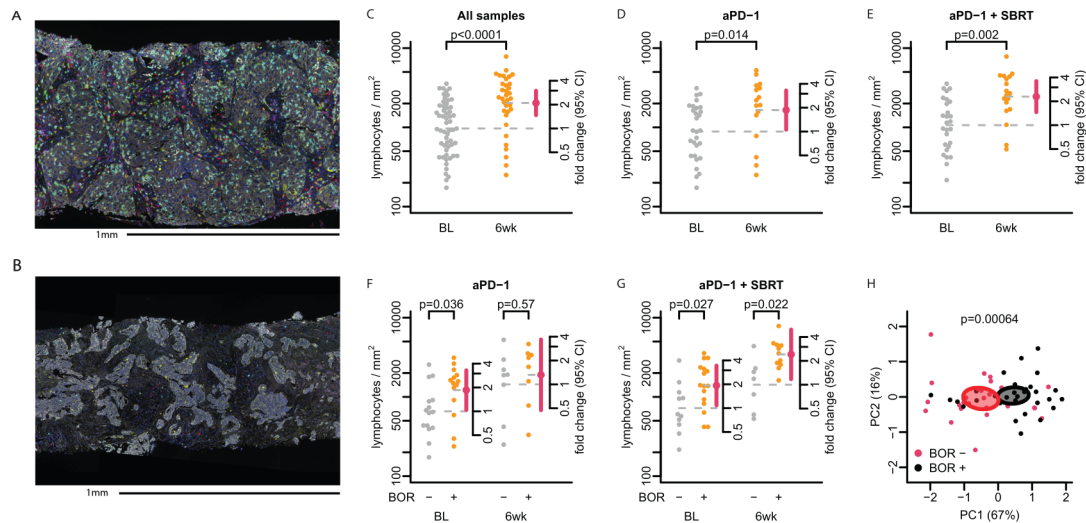


Figure 2 Quantification of total lymphocytes in biopsies obtained at baseline (BL) and after 6 weeks (6 wk) of treatment with anti-PD-1 and anti-PD-1 combined with SBRT. (A) Tumor with a high amount of lymphocytes present within the tumor. (B) Tumor with a low amount of lymphocytes present within the tumor. C–E. Quantification of total lymphocytes per mm^2 . Log-transformed data in all samples as well as per treatment group on BL and on-treatment (6 wk) with red dots indicating the fold change and red bars its 95% CI. The dashed line represents the mean lymphocyte infiltration at BL. (F–G) Quantification of lymphocytes according to best overall response (BOR) with BOR+ defined as complete response, partial response or stable disease for a minimum of 6 wk according to the RECIST V.1.1 criteria. Red dots indicating the fold change and red bars its 95% CI. The dashed line represents the mean lymphocyte infiltration of non-responders. (H) PCA on all BL samples with a difference on PC1 (67% of variance) between patients who respond (BOR+) and do not respond (BOR–), $p=0.00064$ —see also ‘Materials and methods’ section and online supplemental figures 4,5). PC, principal component; PD-1, programmed cell death 1; SBRT, stereotactic body radiation therapy.

more patients with a PD-L1 tumor proportion score of 50% or higher than the anti-PD-1 group (23% vs 13%). Although we observed higher lymphocyte numbers with higher PD-L1 expression, no trend in higher lymphocyte numbers for the anti-PD-L1+SBRT group compared with the anti-PD-L1 alone group was observed (online supplemental figure 4). The total number of lymphocytes present in the TMEs was higher on treatment compared with baseline, an effect that was more pronounced in the anti-PD-1+SBRT group (fold change: 2.29, 95% CI: 1.46 to 3.60, $p<0.0001$) than in the anti-PD-1 group (fold change: 1.87, 95% CI: 1.06 to 3.29, $p=0.014$) (figure 2C–E). To further characterize the association of immune cell infiltrates with response to immunotherapy in pembrolizumab±SBRT-treated patients with NSCLC, we compared immune cell infiltrates at baseline between patients who did and did not respond. Responders (defined as complete response, partial response or stable disease for a minimum of 12 weeks according to the RECIST V.1.1 criteria²⁸) had a significantly higher number of lymphocytes at baseline compared with the non-responders in both the anti-PD-1 group (fold change: 1.86, 95% CI: 1.04 to 3.29 $p=0.036$) as well as in the anti-PD-1+SBRT group (fold change: 1.93, 95% CI: 1.08 to 3.44, $p=0.027$) (figure 2F,G), confirming the link between overall lymphocyte infiltration and favorable patient outcome.

Individual-specific lymphocyte subsets correlated strongly with the total lymphocytic infiltrate (online supplemental figure 5), suggesting that it was mostly the total lymphocyte

pool—rather than a specific subset—that was associated with response to therapy.

However, it is possible that a specific combination of subsets may contain an additional predictive value for response to therapy over total lymphocyte infiltration. To test this hypothesis, we applied PCA on all baseline samples and all tested markers to identify which patients have overall similar immune infiltrates. PCA transforms multiple variables into Cs that explain as much variation in the data as possible. If there are separate groups of patients (ie, a cluster) that score particularly high or low on a set of PCs, these likely have distinct lymphocyte infiltrates that correlate with response to therapy. No clusters or correlations, however, could be identified by PCA. Most of the variation was explained by the first PC, which roughly corresponds with the total number of lymphocytes (PC1, with 67% of the variance, has positive loadings of similar size for all subsets; see online supplemental figure 5). Hence, the PCA analysis confirmed that total lymphocyte infiltration before treatment differs between responders and non-responders (figure 2H, $p=0.00064$). This difference in baseline total lymphocyte infiltrate was more pronounced within the anti-PD-1+SBRT group compared with within the anti-PD-1 group (online supplemental figure 6).

The combination of immunotherapy and irradiation leads to an abscopal effect on the tumor microenvironment

To examine how SBRT alters the immune infiltrate of pembrolizumab-treated patients, we examined the TME

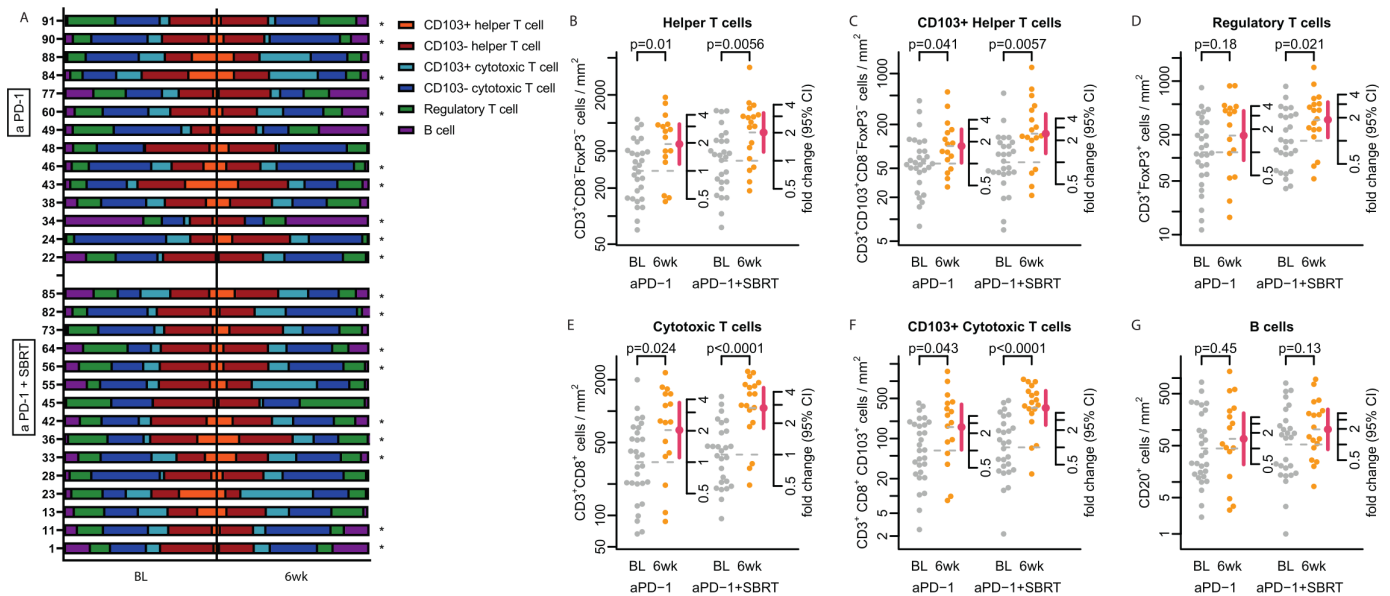


Figure 3 Quantification of lymphocyte subsets in biopsies obtained at baseline (BL) and 6 weeks (6 wk) on-treatment with anti-PD-1 and anti-PD-1 combined with SBRT. (A) Paired samples before and after 6 wk of treatment with relative percentages of lymphocyte subsets. *Patients who clinically responded to therapy. (B–G) Quantification of lymphocyte subsets per mm^2 , log-transformed data, BL versus on-treatment (12 wk), with red dots indicating the fold change and red bars its 95% CI, and p values from Welch's t-test on log-transformed densities (see 'Materials and methods' section). (B) Helper T-cells: aPD-1 fold change: 1.94, 95% CI: 1.19 to 3.18, aPD-1+SBRT fold change: 2.01, 95% CI: 1.24 to 3.25. (C) CD103⁺ helper T-cells: aPD-1 fold change: 1.74, 95% CI: 1.02 to 2.95, aPD-1+SBRT fold change: 2.47, 95% CI: 1.33 to 4.60. (D) Regulatory T-cells: aPD-1 fold change: 1.65, 95% CI: 0.79 to 3.46, aPD-1+SBRT fold change: 1.88, 95% CI: 1.11 to 3.19. (E) Cytotoxic T-cells: aPD-1 fold change: 2.03, 95% CI: 1.11 to 3.72, aPD-1+SBRT fold change: 2.80, 95% CI: 1.79 to 4.38. (F) CD103⁺ cytotoxic T-cells: aPD-1 fold change: 2.56, 95% CI: 1.03 to 6.36, aPD-1+SBRT fold change: 4.87, 95% CI: 2.45 to 9.68. (G) B-cells: aPD-1 fold change: 1.53, 95% CI: 0.49 to 4.77, aPD-1+SBRT fold change: 1.95, 95% CI: 0.81 to 4.74. BOR, best overall response; PD-1, programmed cell death 1; SBRT, stereotactic body radiation therapy.

of non-irradiated tumor sites after 6 weeks of treatment. Total lymphocytic infiltrate increased significantly, irrespective of the addition of SBRT to pembrolizumab, with a fold change of 1.86 (95% CI: 1.06 to 3.29, $p=0.012$) in the anti-PD-1 group (figure 2D), and a fold change of 2.29 (95% CI: 1.46 to 3.60, $p=0.00071$) in the anti-PD-1+SBRT group (figure 2E). The relative contributions of lymphocyte subsets are displayed in figure 3A, per treatment group at baseline and on-treatment of patients for whom matched samples were available ($n=29$). In individual patients, we observed minor shifts in lymphocyte composition in the TME after treatment. However, a clear trend is lacking (figure 3A).

After 6 weeks on-treatment with either anti-PD-1 or anti-PD-1+SBRT, an increase in all lymphocyte-subsets was observed in the TMEs. Significant increases were observed in helper T-cells and cytotoxic T-cells (both CD103⁺ and CD103⁻) in both patient groups, and in regulatory T-cells in biopsies of patients treated with anti-PD-1+SBRT (figure 3B–F). Changes in cell numbers within the TME of patients from whom paired samples were available are shown in online supplemental figure 7.

Notably, although an increase of T-cells on treatment in both the anti-PD-1 and anti-PD-1+SBRT groups was observed, the increase after anti-PD-1+SBRT was consistently higher compared with anti-PD-1 alone (figure 3B–F). For CD103⁺ cytotoxic T-cells specifically,

the fold change was twice as high for anti-PD-1+SBRT compared with anti-PD-1 alone (2.56, 95% CI: 1.03 to 6.36 vs 4.87, 95% CI: 2.45 to 9.68, respectively) (figure 3F). B-cells showed no significant differences between the groups (figure 3G). Thus, although all T-cell populations increased regardless of treatment, both cytotoxic and helper T-cells increased more strongly if anti-PD-1 was combined with SBRT.

Absence of HLA-A/B/C cell surface expression does not impact lymphocyte infiltration in the TME

The presence of lymphocytes in the TME is often ascribed to the recognition of tumor antigens presented on HLA and recognized by specific T-cells. A common hypothesized tumor escape mechanism is the downregulation of HLA class I (HLA-A/B/C). Downregulation by tumor cells of HLA class I prevents tumor recognition by cytotoxic T-cells and subsequent local expansion of T-cells, leading to less lymphocytes in the TME. Absence of HLA-A/B/C on the cell membrane can be caused by downregulation of HLA A/B/C itself or by downregulation of beta-2-microglobulin.²⁹ The reduced infiltration of both cytotoxic T-cells and helper T-cells at baseline and 6 weeks on treatment in non-responding patients was the direct rationale for studying the HLA-A/B/C expression on tumor cells. Strikingly, no differences between tumor samples with HLA-A/B/C or without HLA-A/B/C expression were observed with respect to the number of

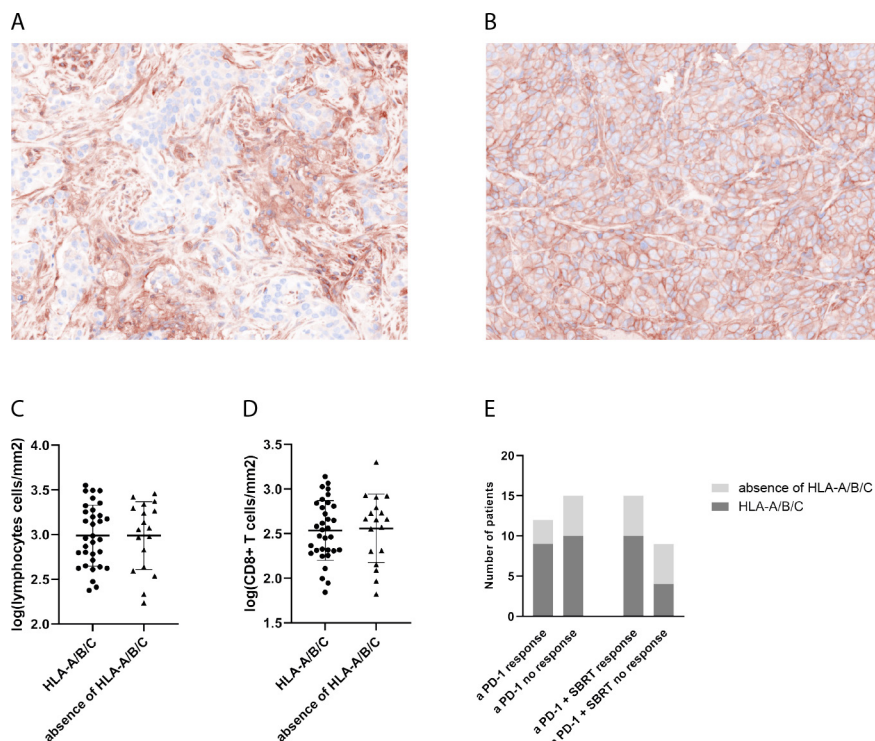


Figure 4 Quantification of HLA-A/B/C and lymphocyte subsets in biopsies obtained at baseline with anti-PD-1 and anti-PD-1 combined with SBRT. (A) Pseudo-DAB image of a tumor with no expression of (membranous) HLA-A/B/C and (B) with membranous expression of HLA-A/B/C. (C) Total lymphocyte counts in patients with and without membranous expression of HLA-A/B/C. (D) CD8⁺ lymphocytes in patients with and without membranous HLA-A/B/C. (E) Quantification of patients with and without expression of HLA-A/B/C per treatment group, divided into responders and non-responders. DAB, 3,3'-diaminobenzidine; PD-1, programmed cell death 1; SBRT, stereotactic body radiation therapy.

total lymphocytes, the number of cytotoxic T-cells or the numbers of any of the other lymphocyte subsets (figure 4). However, patients without tumor cell HLA-A/B/C expression at baseline were less likely to respond to therapy in both the anti-PD-1 group (33% of non-responders and 25% of the responders at baseline lacked expression of HLA-A/B/C on tumor cells) and the anti-PD-1+SBRT group (55% of non-responders and 33% of the responders at baseline lacked tumor cell expression of HLA-A/B/C) (figure 4). Six weeks on-treatment, the change in HLA-A/B/C expression was examined in the paired samples. No clear effect of anti-PD-1 or anti-PD-1+SBRT treatment on the expression of HLA-A/B/C was observed in biopsies of patients with NSCLC (online supplemental figure 8).

DISCUSSION

Here, we used mIF to explore the TME of a unique cohort of patients with NSCLC treated with anti-PD-1 alone or anti-PD-1+SBRT, in which both baseline and 6 weeks on-treatment tissue was available, to investigate the additive effect of SBRT on the anticancer immune response to anti-PD-1 treatment. We found that SBRT, added to anti-PD-1, enhanced the infiltration of all T-cell subsets into the tumor with a nearly 5-times fold change for CD103⁺ cytotoxic T-cells. Anti-PD-1 alone modestly enhanced total and CD103⁺ cytotoxic T-cell infiltration. We also established that overall lymphocyte infiltration

at baseline, but not the presence of any specific lymphocyte subset, is associated with response to therapy in both treatment groups. No relation between the loss of HLA-ABC and the composition of the TME immune infiltrate at baseline was observed. Loss of HLA-ABC was more frequently observed in non-responding patients.

Our observation that combined SBRT and immunotherapy increased T-cell infiltration in tumors of patients with NSCLC might provide evidence for an immunological substantiation for the previously described abscopal effect.⁸ Anti-PD-1 monotherapy also increased T-cell infiltration, but this effect was more pronounced in the anti-PD-1+SBRT group across all subsets.

In non-responding patients, the increase in TME-infiltrating lymphocytes after treatment was higher than in responding patients. Possibly, this bigger increase was due to a lower starting number of lymphocytes, and despite the increase, failing to reach a threshold for an effect. Whereas in responding patients a smaller increase in lymphocyte numbers could be sufficient to get an effect or the lymphocytes present at baseline are reinvigorated due to the PD-1 treatment. The abscopal effect of radiotherapy has been attributed to the activation of the immune system by irradiation-induced breakdown products of tumor cells within the irradiated lesion.^{8 30 31} In a preclinical model of colorectal cancer, radiotherapy induced upregulation of the maturation markers CD80

and CD86 on DCs, and an increase in CD8⁺ T-cells within the TME was observed.³² In a NSCLC xenograft mouse model, radiotherapy increased PD-L1 expression and CD8⁺ T-cell infiltration.¹³ Furthermore, there was a synergistic effect of anti-PD-L1 therapy and radiotherapy: in mouse models, tumor regression and MDSC reduction were observed.^{13 33} An increase in cytotoxic T-cells in patients with NSCLC treated with radiotherapy alone has been observed as well,^{34 35} but to our knowledge, we are the first to establish this effect in a randomized patient cohort receiving anti-PD-1 therapy with or without SBRT. These immunological data show how SBRT can be of added value as an important component in immunotherapy combination strategies. It would be interesting to functionally characterize the tumor T-cell compartment since it is known that the phenotype and function of T-cells can differ.^{36 37} This could elucidate the functional implications of the T-cell compartment changes that we observed. Unfortunately, this is practically very challenging in human clinical research.

As previously described, tumor samples can be categorized as hot, immune excluded or desert depending on the presence, location or absence of an immune cell infiltrate.^{38 39} However, in our cohort only the distinction hot or desert could be made since in the available biopsy material invasive margins cannot be reliably detected. Furthermore, the number as opposed to the location of immune cells was associated with the overall survival of patients with NSCLC and their response to immunotherapy.⁴⁰ However, study results have been contradicting, and multiple candidate immune cells are suggested as the key player in facilitating a response to anti-PD-1 therapy.^{41–43} α_E -integrin CD103 has been used as a marker to identify tumor-infiltrating lymphocytes.⁴⁴ Furthermore, CD103⁺CD8⁺ T-cells in the human lung have been shown to possess a greater cytotoxic potential than other CD8⁺ T-cells.^{26 45} In NSCLC, the relative amount of this subset in tumor samples correlated with disease-free survival in early stage disease.⁴⁶ Furthermore, a high number of CD103-expressing cells in the tumor, on both gene expression and protein level, was associated with longer overall survival in patients with NSCLC treated with anti-PD-L1 immunotherapy (17.9 months in CD103⁺ high patients compared with 9.5 months in CD103⁺ low).⁴⁷ In another study, CD103⁺CD8⁺ T-cell infiltration in NSCLC tumors strongly correlated with progression-free survival (PFS) after immunotherapy (30 months in CD103⁺CD8⁺ high patients and 2.3 months in CD103⁺CD8⁺ low patients). Specifically, PFS in patients with high numbers of CD103⁺CD8⁺ was 20 months longer than in patients with high numbers of CD8⁺ T-cells.⁴⁸ Therefore, we characterized this specific subset in our panel and confirmed that responding patients have more CD103⁺ CD8⁺ T-cells in their TME. However, the CD103⁺ CD8⁺ T-cell subset was increased in responding patients at baseline, and the other subsets. Further analyses of this observation with PCA indicated that a higher number of lymphocytes in general—and not a particular subset—was associated

with response to therapy. It should be noted that the mIF employed in this study only allows for a limited set of markers; therefore, only broad subsets of T-cells could be identified. When searching for a biomarker to predict response to immunotherapy, it is likely that not a single marker but a set of markers is required.⁴⁹ Total lymphocyte infiltration and tumor-intrinsic factors could relatively easily be incorporated into such a multifactorial biomarker.

Radiotherapy can induce HLA-ABC expression on tumor cells.¹⁵ We did not observe an effect of anti-PD-1 alone or anti-PD-1 with SBRT on HLA-ABC expression. Possible explanations for this are that the effect of SBRT on the expression of HLA-ABC only occurs in the irradiated lesion, that the effect is not substantiated due to the small number of paired samples or that the biopsy was taken too early in the process. Furthermore, radiation dose, fractionation and interval might influence the immunological effect. Expression of HLA-ABC on tumor cells is vital for tumor antigen presentation and recognition by cytotoxic T-cells, and thereby absence of HLA-ABC expression prevents tumor destruction.^{50 51} Indeed, at baseline, a slightly larger percentage of patients with absence of HLA-ABC among non-responding patients was observed, although the significance of this finding could not be established in this small sample size. No relationship between HLA-ABC expression and the number of tumor-infiltrating lymphocytes or any lymphocyte subset was observed. The mechanism of immune evasion by absence of membranous HLA-ABC, however, is not straightforward. In a cohort of patients with melanoma, no relation was found between absence of HLA-ABC and response to immunotherapy. Impaired HLA-ABC may play a more important role in acquiring resistance to ICI therapy.²⁹ The Tracking Non-Small-Cell Lung Cancer Evolution through Therapy (TRACERx) study showed that impairment of HLA is often caused by loss of heterozygosity and is a mutation that occurs late in tumor evolution, complicating the recognition of tumor subclones by T-cells.⁵² On the other hand, we observed the reoccurrence of HLA-ABC expression after 6 weeks on treatment in some patients. This could be due to IFN production by PD-L1-re-activated T cells. This clonal heterogeneity and the continued interplay between a tumor and the immune system might become a focus for future research into durable responses to immunotherapy.⁵³

The treatment of advanced-stage NSCLC has evolved in the last decade from chemotherapy, with radiotherapy for symptom relief, to treatment with targeted therapy and immunotherapy. Because not all patients benefit from immunotherapy, strategies to overcome immunotherapy resistance are being investigated. A combination with radiotherapy is one promising strategy that is being explored. Despite the small size of this cohort, valuable information about the effect of treatment on the TME could be obtained. Our data demonstrate differences in total lymphocytic infiltrate between responding and non-responding patients at baseline. More importantly,

our study demonstrates an immunological abscopal effect of the SBRT and anti-PD-1 therapy combination. The abscopal effect of radiotherapy alone is rare. It is believed that most of the time, tumors employ suppressive mechanisms to counteract an increase of primed T-cells. We believe that combining radiotherapy with immunotherapy can overcome this suppressive effect of the tumor, allowing for an increase of T-cells at distant, non-irradiated tumor sites. Further clinical investigation is warranted to confirm this effect in an extended clinical trial for future implementation of this promising strategy.

Author affiliations

¹Department of Tumour Immunology, Radboudumc, Nijmegen, The Netherlands

²Department of Pathology, Radboudumc, Nijmegen, The Netherlands

³Division of Immunotherapy, Oncode Institute, Radboudumc, Nijmegen, the Netherlands

⁴Data Science, Institute for Computing and Information Sciences, Radboud University, Nijmegen, the Netherlands

⁵Department of Pathology, Netherlands Cancer Institute, Amsterdam, The Netherlands

⁶Department of Pulmonary Diseases, Radboudumc, Nijmegen, The Netherlands

⁷Department of Pulmonology, Netherlands Cancer Institute, Amsterdam, The Netherlands

Acknowledgements We wish to thank the study investigators, site staff, the participants and their families who participated in this study. We want to thank pathologist Monika Looijen-Salamon (ML) for her help assessing the tumor specimens. We would also like to acknowledge the NKI-AVL Core Facility Molecular Pathology & Biobanking (CFMPB) for supplying Biobank material and laboratory support.

Contributors Concept and design: LLvdW, WSMET, BP. Execution of experiments: LLvdW, KV. Analysis and interpretation: LLvdW, WSMET, MAJG, JHAC, IMNW, JT, KG, IJMdV and BP. Drafting of the manuscript: LLvdW, BP. Critical revision of the manuscript for important intellectual content: all authors. Supervision: IJMdV, BP. Guarantor: IJMdV.

Funding This study was an investigator-initiated trial, designed by the authors and financially supported by Dutch Cancer Society grant 10673 and an unrestricted grant from Merck Sharp & Dohme that included medication supply.

Competing interests WSMET reports grants from AstraZeneca, MSD and Sanofi.

Patient consent for publication Not applicable.

Ethics approval This study was approved by Ethics Committee of the Netherlands Cancer Institute—Antoni van Leeuwenhoek Hospital, Amsterdam (NCT02492568). The trial was conducted in accordance with the provisions of the Declaration of Helsinki and the Good Clinical Practice Guidelines of the European Medicines Agency and the US Food and Drug Administration. Participants gave informed consent to participate in the study before taking part.

Provenance and peer review Not commissioned; externally peer reviewed.

Data availability statement Data are available on reasonable request.

Supplemental material This content has been supplied by the author(s). It has not been vetted by BMJ Publishing Group Limited (BMJ) and may not have been peer-reviewed. Any opinions or recommendations discussed are solely those of the author(s) and are not endorsed by BMJ. BMJ disclaims all liability and responsibility arising from any reliance placed on the content. Where the content includes any translated material, BMJ does not warrant the accuracy and reliability of the translations (including but not limited to local regulations, clinical guidelines, terminology, drug names and drug dosages), and is not responsible for any error and/or omissions arising from translation and adaptation or otherwise.

Open access This is an open access article distributed in accordance with the Creative Commons Attribution Non Commercial (CC BY-NC 4.0) license, which permits others to distribute, remix, adapt, build upon this work non-commercially, and license their derivative works on different terms, provided the original work is properly cited, appropriate credit is given, any changes made indicated, and the use is non-commercial. See <http://creativecommons.org/licenses/by-nc/4.0/>.

ORCID iDs

Lieke L van der Woude <http://orcid.org/0000-0002-4761-0768>

Mark A J Gorris <http://orcid.org/0000-0003-3621-226X>

Jeroen H A Creemers <http://orcid.org/0000-0003-0371-8416>

Kiek Verrijp <http://orcid.org/0000-0001-5223-8406>

Johannes Textor <http://orcid.org/0000-0002-0459-9458>

Carl G Figdor <http://orcid.org/0000-0002-2366-9212>

I Jolanda M de Vries <http://orcid.org/0000-0002-8653-4040>

REFERENCES

- Doroshov DB, Sanmamed MF, Hastings K, *et al*. Immunotherapy in non-small cell lung cancer: facts and hopes. *Clin Cancer Res* 2019;25:4592–602.
- Genova C, Rossi G, Tagliamento M, *et al*. Targeted therapy of oncogenic-driven advanced non-small cell lung cancer: recent advances and new perspectives. *Expert Rev Respir Med* 2020;14:367–83.
- Reck M, Rodríguez-Abreu D, Robinson AG, *et al*. Pembrolizumab versus chemotherapy for PD-L1-positive non-small-cell lung cancer. *N Engl J Med* 2016;375:1823–33.
- Herbst RS, Baas P, Kim D-W, *et al*. Pembrolizumab versus docetaxel for previously treated, PD-L1-positive, advanced non-small-cell lung cancer (KEYNOTE-010): a randomised controlled trial. *Lancet* 2016;387:1540–50.
- Garon EB, Hellmann MD, Rizvi NA, *et al*. Five-Year overall survival for patients with advanced Non-Small-Cell lung cancer treated with pembrolizumab: results from the phase I KEYNOTE-001 study. *J Clin Oncol* 2019;37:2518–27.
- Bodor JN, Boumber Y, Borghaei H. Biomarkers for immune checkpoint inhibition in non-small cell lung cancer (NSCLC). *Cancer* 2020;126:260–70.
- Garelli E, Rittmeyer A, Putora PM, *et al*. Abscopal effect in lung cancer: three case reports and a Concise review. *Immunotherapy* 2019;11:1445–61.
- Rodríguez-Ruiz ME, Vanpouille-Box C, Melero I, *et al*. Immunological mechanisms responsible for radiation-induced Abscopal effect. *Trends Immunol* 2018;39:644–55.
- Harding SM, Benci JL, Irianto J, *et al*. Mitotic progression following DNA damage enables pattern recognition within micronuclei. *Nature* 2017;548:466–70.
- Apetoh L, Ghiringhelli F, Tesniere A, *et al*. Toll-like receptor 4-dependent contribution of the immune system to anticancer chemotherapy and radiotherapy. *Nat Med* 2007;13:1050–9.
- Wu Q, Allouch A, Martins I, *et al*. Macrophage biology plays a central role during ionizing radiation-elicited tumor response. *Biomed J* 2017;40:200–11.
- Dovedi SJ, Adlard AL, Lipowska-Bhalla G, *et al*. Acquired resistance to fractionated radiotherapy can be overcome by concurrent PD-L1 blockade. *Cancer Res* 2014;74:5458–68.
- Gong X, Li X, Jiang T, *et al*. Combined radiotherapy and anti-PD-L1 antibody synergistically enhances antitumor effect in non-small cell lung cancer. *J Thorac Oncol* 2017;12:1085–97.
- Klug F, Prakash H, Huber PE, *et al*. Low-dose irradiation programs macrophage differentiation to an iNOS⁺/M1 phenotype that orchestrates effective T cell immunotherapy. *Cancer Cell* 2013;24:589–602.
- Reits EA, Hodge JW, Herberts CA, *et al*. Radiation modulates the peptide repertoire, enhances MHC class I expression, and induces successful antitumor immunotherapy. *J Exp Med* 2006;203:1259–71.
- Theelen WSME, Peulen HMU, Lalezari F, *et al*. Effect of pembrolizumab after stereotactic body radiotherapy vs pembrolizumab alone on tumor response in patients with advanced non-small cell lung cancer: results of the PEMBRO-RT phase 2 randomized clinical trial. *JAMA Oncol* 2019;5:1276–1282.
- Lin AJ, Roach M, Bradley J, *et al*. Combining stereotactic body radiation therapy with immunotherapy: current data and future directions. *Transl Lung Cancer Res* 2019;8:107–15.
- Lazzari C, Karachaliou N, Bulotta A, *et al*. Combination of immunotherapy with chemotherapy and radiotherapy in lung cancer: is this the beginning of the end for cancer? *Ther Adv Med Oncol* 2018;10:1758835918762094.
- World Medical Association Declaration of Helsinki. Ethical principles for medical research involving human subjects. *Jama* 2013;310:2191–4.
- Gorris MAJ, Halilovic A, Rabold K, *et al*. Eight-Color multiplex immunohistochemistry for simultaneous detection of multiple immune checkpoint molecules within the tumor microenvironment. *J Immunol* 2018;200:347–54.

- 21 Sultan Set *et al.* A Segmentation-Free machine learning architecture for immune Land-scape phenotyping in solid tumors by multichannel imaging. *bioRxiv* 2021.
- 22 Gamer M, Lemon J, Fellows I. irr: Various coefficients of interrater reliability and agreement [computer software] 2012.
- 23 Ho J, Tumkaya T, Aryal S, *et al.* Moving beyond P values: data analysis with estimation graphics. *Nat Methods* 2019;16:565–6.
- 24 Stankovic B, Bjørhovde HAK, Skarshaug R, *et al.* Immune cell composition in human non-small cell lung cancer. *Front Immunol* 2018;9:3101.
- 25 Pyszniak M, Rybojad P, Pogoda K, *et al.* Percentages of NKT cells in the tissues of patients with non-small cell lung cancer who underwent surgical treatment. *Kardiochir Torakochirurgia Pol* 2014;11:34–9.
- 26 Hombrink P, Helbig C, Backer RA, *et al.* Programs for the persistence, vigilance and control of human CD8⁺ lung-resident memory T cells. *Nat Immunol* 2016;17:1467–78.
- 27 Fridman WH, Pagès F, Sautès-Fridman C, *et al.* The immune contexture in human tumours: impact on clinical outcome. *Nat Rev Cancer* 2012;12:298–306.
- 28 Eisenhauer EA, Therasse P, Bogaerts J, *et al.* New response evaluation criteria in solid tumours: revised RECIST guideline (version 1.1). *Eur J Cancer* 2009;45:228–47.
- 29 Gettinger S, Choi J, Hastings K, *et al.* Impaired HLA class I antigen processing and presentation as a mechanism of acquired resistance to immune checkpoint inhibitors in lung cancer. *Cancer Discov* 2017;7:1420–35.
- 30 Popp I, Grosu AL, Niedermann G, *et al.* Immune modulation by hypofractionated stereotactic radiation therapy: therapeutic implications. *Radiother Oncol* 2016;120:185–94.
- 31 Shahabi V, Postow MA, Tuck D, *et al.* Immune-priming of the tumor microenvironment by radiotherapy: rationale for combination with immunotherapy to improve anticancer efficacy. *Am J Clin Oncol* 2015;38:90–7.
- 32 Frey B, Rückert M, Weber J, *et al.* Hypofractionated irradiation has immune stimulatory potential and induces a timely restricted infiltration of immune cells in colon cancer tumors. *Front Immunol* 2017;8:231.
- 33 Deng L, Liang H, Burnette B, *et al.* Irradiation and anti-PD-L1 treatment synergistically promote antitumor immunity in mice. *J Clin Invest* 2014;124:687–95.
- 34 Zheng Y, Shi A, Wang W, *et al.* Posttreatment immune parameters predict cancer control and pneumonitis in stage I non-small-cell lung cancer patients treated with stereotactic ablative radiotherapy. *Clin Lung Cancer* 2018;19:e399–404.
- 35 Zeng H, Zhang W, Gong Y, *et al.* Radiotherapy activates autophagy to increase CD8⁺ T cell infiltration by modulating major histocompatibility complex class-I expression in non-small cell lung cancer. *J Int Med Res* 2019;47:3818–30.
- 36 Oja AE, Piet B, van der Zwan D, *et al.* Functional Heterogeneity of CD4⁺ Tumor-Infiltrating Lymphocytes With a Resident Memory Phenotype in NSCLC. *Front Immunol* 2018;9:2654.
- 37 Wherry EJ, Kurachi M. Molecular and cellular insights into T cell exhaustion. *Nat Rev Immunol* 2015;15:486–99.
- 38 Hegde PS, Karanikas V, Evers S. The where, the when, and the how of immune monitoring for cancer immunotherapies in the era of checkpoint inhibition. *Clin Cancer Res* 2016;22:1865–74.
- 39 van der Woude LL, Gorris MAJ, Halilovic A, *et al.* Migrating into the tumor: a roadmap for T cells. *Trends Cancer* 2017;3:797–808.
- 40 Prelaj A, Tay R, Ferrara R, *et al.* Predictive biomarkers of response for immune checkpoint inhibitors in non-small-cell lung cancer. *Eur J Cancer* 2019;106:144–59.
- 41 Al-Shibli KI, Donnem T, Al-Saad S, *et al.* Prognostic effect of epithelial and stromal lymphocyte infiltration in non-small cell lung cancer. *Clin Cancer Res* 2008;14:5220–7.
- 42 Kawai O, Ishii G, Kubota K, *et al.* Predominant infiltration of macrophages and CD8(+) T Cells in cancer nests is a significant predictor of survival in stage IV nonsmall cell lung cancer. *Cancer* 2008;113:1387–95.
- 43 Wakabayashi O, Yamazaki K, Oizumi S, *et al.* Cd4+ T cells in cancer stroma, not CD8+ T cells in cancer cell nests, are associated with favorable prognosis in human non-small cell lung cancers. *Cancer Sci* 2003;94:1003–9.
- 44 Smazynski J, Webb JR. Resident Memory-Like Tumor-Infiltrating Lymphocytes (TIL_{RM}): Latest Players in the Immuno-Oncology Repertoire. *Front Immunol* 2018;9:1741.
- 45 Piet B, de Bree GJ, Smids-Dierdorp BS, *et al.* Cd8⁺ T cells with an intraepithelial phenotype upregulate cytotoxic function upon influenza infection in human lung. *J Clin Invest* 2011;121:2254–63.
- 46 Djenidi F, Adam J, Goubar A, *et al.* CD8+CD103+ tumor-infiltrating lymphocytes are tumor-specific tissue-resident memory T cells and a prognostic factor for survival in lung cancer patients. *J Immunol* 2015;194: :3475–86.
- 47 Banchereau R, Chitre AS, Scherl A, *et al.* Intratumoral CD103+ CD8+ T cells predict response to PD-L1 blockade. *J Immunother Cancer* 2021;9.
- 48 Corgnac S, Malenica I, Mezquita L, *et al.* CD103⁺CD8⁺ T_{RM} Cells Accumulate in Tumors of Anti-PD-1-Responder Lung Cancer Patients and Are Tumor-Reactive Lymphocytes Enriched with Tc17. *Cell Rep Med* 2020;1:100127.
- 49 Hegde PS, Chen DS. Top 10 challenges in cancer immunotherapy. *Immunity* 2020;52:17–35.
- 50 Sade-Feldman M, Jiao YJ, Chen JH, *et al.* Resistance to checkpoint blockade therapy through inactivation of antigen presentation. *Nat Commun* 2017;8:1136.
- 51 Perea F, Sánchez-Palencia A, Gómez-Morales M, *et al.* Hla class I loss and PD-L1 expression in lung cancer: impact on T-cell infiltration and immune escape. *Oncotarget* 2018;9:4120–33.
- 52 Jamal-Hanjani M, Wilson GA, McGranahan N, *et al.* Tracking the evolution of non-small-cell lung cancer. *N Engl J Med* 2017;376:2109–21.
- 53 Wu Y, Biswas D, Swanton C. Impact of cancer evolution on immune surveillance and checkpoint inhibitor response. *Semin Cancer Biol* 2022;32:89–102.